



ELSEVIER

Available at
www.ComputerScienceWeb.com
POWERED BY SCIENCE @ DIRECT®

COMPUTER
AIDED
GEOMETRIC
DESIGN

Computer Aided Geometric Design 20 (2003) 319–341

www.elsevier.com/locate/cagd

On the angular defect of triangulations and the pointwise approximation of curvatures[☆]

V. Borrelli^a, F. Cazals^{b,*}, J.-M. Morvan^{a,b}

^a Institut Girard Desargues, Univ. Lyon I, Mathematiques, 43 Boulevard du 11 Novembre 1918, F-69622 Villeurbanne, France

^b INRIA Sophia-Antipolis, 2004 route des Lucioles, F-06902 Sophia-Antipolis, France

Received 17 October 2002; received in revised form 16 April 2003; accepted 24 April 2003

Abstract

Let S be a smooth surface of E^3 , p a point on S , k_m , k_M , k_G and k_H the maximum, minimum, Gauss and mean curvatures of S at p . Consider a set $\{p_i p_{i+1}\}_{i=1,\dots,n}$ of n Euclidean triangles forming a piecewise linear approximation of S around p —with $p_{n+1} = p_1$. For each triangle, let γ_i be the angle $\angle p_i p p_{i+1}$, and let the angular defect at p be $2\pi - \sum_i \gamma_i$. This paper establishes, when the distances $\|pp_i\|$ go to zero, that the angular defect is asymptotically equivalent to a homogeneous polynomial of degree two in the principal curvatures.

For regular meshes, we provide closed forms expressions for the three coefficients of this polynomial. We show that vertices of valence four and six are the only ones where k_G can be inferred from the angular defect. At other vertices, we show that the principal curvatures can be derived from the angular defects of two independent triangulations. For irregular meshes, we show that the angular defect weighted by the so-called module of the mesh estimates k_G within an error bound depending upon k_m and k_M .

Meshes are ubiquitous in Computer Graphics and Computer Aided Design, and a significant number of papers advocate the use of normalized angular defects to estimate the Gauss curvature of smooth surfaces. We show that the statements made in these papers are erroneous in general, although they may be true pointwise for very specific meshes. A direct consequence is that normalized angular defects should be used to estimate the Gauss curvature for these cases only where the geometry of the meshes processed is precisely controlled. On a more general perspective, we believe this contributions is one step forward the intelligence of the geometry of meshes, whence one step forward more robust algorithms.

© 2003 Elsevier B.V. All rights reserved.

Keywords: Smooth surfaces; Meshes; Curvatures; Approximations; Differential geometry

[☆] Partially supported by the *Effective Computational Geometry for Curves and Surfaces* European project, Project No IST-2000-26473.

* Corresponding author.
E-mail addresses: borrelli@desargues.univ-lyon1.fr (V. Borrelli), frederic.cazals@inria.fr (F. Cazals), Jean-Marie.Morvan@inria.fr (J.-M. Morvan).

1. Introduction

1.1. Smooth and triangulated surfaces

Meshes are ubiquitous in modern computer-related geometry. Meshes are easily obtained from physical objects through scanning and reconstruction. Meshes are commonly displayed by graphical hardware. Meshes are intuitive to deal with. They provide hierarchical representations that can be used for approximate representations. Meshes can be refined to smooth surfaces through subdivision.

In this context, and especially since meshes can be made dense enough so as to “look like” smooth surfaces, it is tempting to define a differential geometry of meshes which mimics that of smooth surfaces.

Example quantities well defined smooth surfaces that also look appealing for meshes are the surface area, the normal vector field, the curvatures, geodesics, the focal sets, the ridges, the medial axis, etc.

Interestingly, recent research in applied domains provides, for each of the notions just enumerated, several estimates adapted from classical differential geometry to the setting of piecewise linear surfaces. Several definitions of normals, principal directions and curvatures over a mesh can be found in (Taubin, 1995; Meyer et al., 2002). Ridges of polyhedral surfaces as well as cuspidal edges of the focal sets are computed in (Watanabe and Belyaev, 2001). Geodesics and discrete versions of the Gauss–Bonnet theorem are considered in (Polthier and Schmies, 1998). But none of these contributions address the question of the accuracy of these estimates or that of their convergence when the mesh is refined.

As opposed to these approaches, the literature provides a few examples of *a priori* analysis. Given a discrete set—a point cloud or a mesh—which is assumed to sample a surface in a certain way, differential operators are derived together with theoretical guarantees about the discrepancy between the discrete estimates and the true value on the underlying smooth surface.

In (Amenta and Bern, 1999) it is shown that the normal to a smooth surface sampled according to a criterion involving the skeleton can be estimated accurately from the Voronoi diagram of the sample points. The surface area of a mesh and its normal vector field versus those of a smooth surface are considered in (Morvan and Thibert, 2001). More closely related to the question we address is (Meek and Walton, 2000), which provides some error bounds for estimates of the normal and the Gauss curvature of a sampled surface. In particular, Meek and Walton observe on a counterexample that the angular defect does not estimate the Gauss curvature, but no analysis is carried out. The missing analysis is presented in this paper.

1.2. Smooth surfaces, polyhedra, Gauss curvature and angular defect

In this section, we highlight striking parallels between the Gauss curvature of polyhedra and smooth surfaces of E^3 . More precisely, we recall:

- (1) the definition of the Gauss curvature for smooth surfaces and polyhedra, as well as the Gauss–Bonnet theorem in both cases.
- (2) how the Gauss curvature of a smooth surface can be recovered from the angular defect of geodesic triangles.

1.2.1. Gauss curvature and the Gauss–Bonnet theorem for surfaces and polyhedra

The Gauss curvature of an (abstract) oriented smooth Riemannian surface M is a smooth function k_G on M defined by using the metric tensor. It is well known that the Gauss curvature of a domain is

identically equal to zero if and only if it is locally isometric to a portion of plane. One can associate to k_G a curvature measure K_G on M by integration over any domain U of M :

$$K_G(U) = \int_U k_G da,$$

where da denotes the area form of M . Suppose now that M is isometrically embedded in E^3 . One way to evaluate its Gauss curvature at a point p is to make the product of the two principal curvatures of M at p (this is nothing but *theorema egregium* of Gauss). An equivalent way it to use the Gauss map of the embedding and to calculate the limit A'/A , where A is the surface area of a region around p , A' the signed area of the image of A on S^2 by the Gauss map, the limit being taken (*roughly speaking*) as the region A around p becomes smaller and smaller (Spivak, 1999, Vol. 2, Chapter III).

Consider now an abstract Riemannian polyhedron P . Any point of P which is not a vertex has a neighborhood isometric to a plane, and one can define its Gauss curvature to be 0, by analogy with the smooth case. Moreover, if p is a vertex of P , one can assign to p the angular defect $\alpha_p = 2\pi - \sum_i \gamma_i$ at p , where the γ_i s stand for the angles at p of the facets incident to p . We call this angular defect *the Gauss curvature $k_G(p)$ of the vertex p* (Reshetnyak, 1993, Section 5). Remark that it is now possible to define a curvature measure on P , as a measure concentrated on the vertices of P , by setting over any domain U of P

$$K_G(U) = \sum_{p \text{ vertex in } U} \alpha(p).$$

If P is isometrically embedded in E^3 , then this angular defect is exactly the signed area of the image on S^2 by the Gauss map of any arbitrarily small neighborhood of p , which is a property analogous to the smooth case.

An important relationship relating the Gauss curvature to topological properties is the Gauss–Bonnet theorem. Consider a closed orientable surface S and a closed polyhedron P , the latter with vertices p_1, \dots, p_n . Let $\chi(S)$ and $\chi(P)$ stand for their Euler characteristic—that is $V - E + F$ in the usual jargon. The global Gauss–Bonnet theorem respectively states for S and P that—for the polyhedral case, see (Banchoff, 1967):

$$2\pi \chi(S) = \iint_S k_G d\sigma, \tag{1}$$

$$2\pi \chi(P) = \sum_{i=1, \dots, n} k_G(p_i). \tag{2}$$

These remarkable results actually state that if the topology is fixed—i.e., the genus of the surface or the polyhedron is given, the curvature distributes itself on S or P so as to comply with that topology. Notice that local versions of both theorems exist. (For the geodesic curvature involved in the local Gauss–Bonnet theorem, see (Reshetnyak, 1993; Polthier and Schmies, 1998).)

Remark that in this context, the Gauss curvature of a point of a polyhedron is dimensionless, while that of a surface is homogeneous to the inverse of a surface area. The topological invariant $2\pi \chi$ is dimensionless, which is coherent with Eqs. (1) and (2).

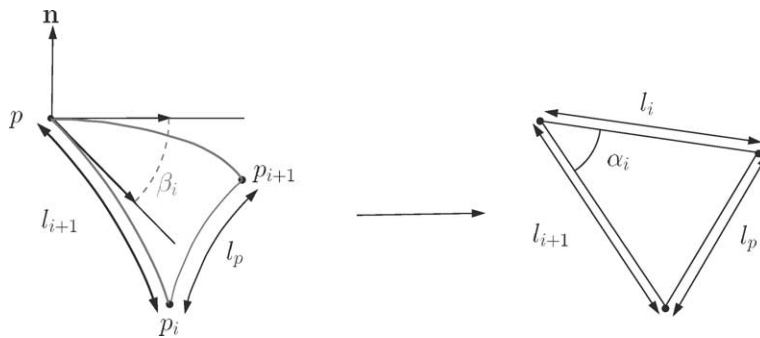


Fig. 1. Flattening a geodesic triangle yields an estimate for the Gauss curvature.

1.2.2. Gauss curvature and geodesic triangles

An important property of geodesic triangles also which involves the Gauss curvature is the following—see (Cheeger et al., 1984; Lafontaine, 1986).

Let τ_i be a geodesic triangle on S , p , p_i and p_{i+1} its vertices, l_p, l_i, l_{i+1} the lengths of the geodesic arcs opposite to the vertices, and $l = \sup\{l_i, l_{i+1}\}$. Let T_i be the Euclidean triangle whose edges have the same lengths as those of τ_i . We call T_i a *Euclidean geodesic triangle* since it is a Euclidean triangle, but its edges' lengths are geodesic distances. Finally, let β_i be the angle of τ_i at p , and α_i be the angle $\angle p_i p p_{i+1}$ of T_i . See Fig. 1 for an illustration. The angles β_i and α_i differ by a term involving the Gauss curvature k_G at p . More precisely, we have

Proposition 1. *The angles β_i and α_i associated to a Euclidean geodesic triangle τ_i satisfy*

$$\beta_i = \alpha_i + \frac{1}{6} \sin \alpha_i k_G l_{i+1} + o(l^2). \quad (3)$$

Consider now a geodesic triangulation around p , that is a set of n geodesic triangles having p as common vertex and forming a topological disk around p . By looking at the tangents to the geodesics from p to the p_i s, we have $\sum_i \beta_i = 2\pi$. Summing Eq. (3) for the n geodesic triangles immediately yields the following

Theorem 1. *Let \mathcal{T} be a geodesic triangulation of a smooth surface M of E^3 . Let p be a vertex of \mathcal{T} , and let $A(p)$ be the sum of the areas of the triangles T_i associated to the Euclidean geodesic triangles τ_i s. Then*

$$2\pi - \sum_i \alpha_i = \frac{A(p)}{3} k_G + o(l^2).$$

This result is of little help from a practical standpoint since the knowledge of geodesics is required. The question addressed in this paper is actually to study the quantity estimated by the angular defect when one replaces the geodesics by the Euclidean line-segments pp_i .

1.3. Question addressed in this paper

Let S be a surface of E^3 , and let p be a point of S . Also suppose that we are given a set $\{p_i p p_{i+1}\}_{i=1, \dots, n}$ of n Euclidean triangles forming a piecewise linear approximation of S around p . We shall refer to these

triangles as the mesh, and to the p_i s as the one-ring neighbors of p . For each triangle, let γ_i be the angle $\angle p_i p p_{i+1}$, and let the angular defect at p be $2\pi - \sum_i \gamma_i$. Also, for a one-ring neighbor p_i , let η_i stand for the Euclidean distance between p and p_i .

The question we address in this paper is:

How precisely can one estimate the curvatures at a point p of a smooth surface using the angular defect of the triangles surrounding p ?

Before presenting the contributions, several comments are in order.

Dimensionality. In order for the previous question to make sense, we shall pay a special attention to the dimensionality of the quantities involved. As already pointed out, the Gauss curvature of a smooth surface is homogeneous to the inverse of a surface area while that of a polyhedron is dimensionless. To estimate the curvatures of a smooth surface from a polyhedron, we will therefore have to normalize by lengths (for the principal curvatures) or surface areas (Gauss curvature).

Smooth surfaces and asymptotic estimates. Estimating the curvatures of a smooth surface S from a single mesh is obviously an hopeless target. The folds of S may indeed occur at a resolution much lower than that of the triangulation, so that the mesh may fall short from providing accurate information on the point-wise curvatures. The problem becomes more tractable if one assumes S belongs to a restricted class of surfaces—e.g., with Lipschitz like conditions on the variation of the normal—or assumes that a sequence of meshes with edges' lengths going to zero is available. We shall in the paper follow this latter perspective and derive asymptotic results.

Soundness of the angular defect for the Gauss curvature of smooth surfaces. Since the angular defect over geodesic triangles provides an estimate of k_G , it is tempting to believe that when the edges lengths $\|pp_i\|$ go to zero, one can safely replace the geodesic arcs from p to the p_i s on S by the Euclidean segments pp_i s. We shall see it is not so.

1.4. Contributions

This paper establishes, when the distances $\|pp_i\|$ go to zero, that the angular defect is asymptotically equivalent to a homogeneous polynomial of degree two in the principal curvatures. To state the results

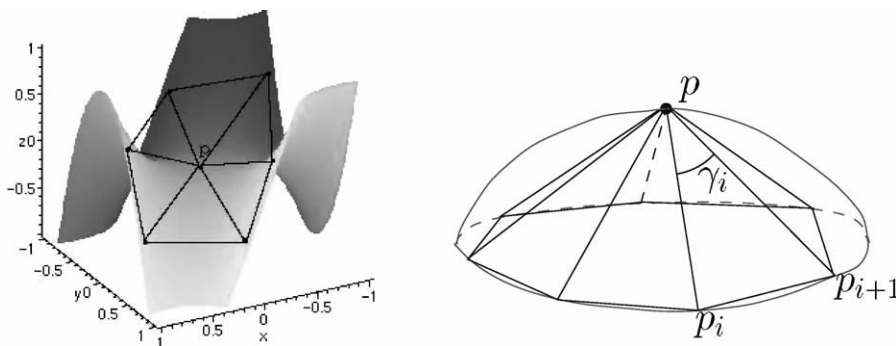


Fig. 2. Can the curvatures of a smooth surface be estimated from the angular defect of a triangulation?

more precisely, one need to distinguish between regular and irregular meshes. By regular mesh, we refer to a mesh such that the p_i s lie in normal sections two consecutive of which form an angle of $2\pi/n$, with the additional constraint that $\|pp_i\|$ is a constant. A mesh which is not regular is called irregular.

Regular meshes. We provide the closed form expression of the afore-mentioned polynomial as a function of the principal curvatures and $2\pi/n$. In particular, we show that $n = 4$ is the only value of n such that $2\pi - \sum_i \gamma_i$ depends upon the principal directions, and that $n = 6$ is the only value such that $2\pi - \sum_i \gamma_i$ provides an exact estimate for k_G . A corollary of these results is that the principal curvatures—whence k_G and k_H —can be computed from the angular defects of any two triangulations whose valences are not four.

Irregular meshes. We show that the angular defect weighted by the so-called module of the mesh estimates k_G within an error bound depending upon k_m and k_M .

Practical relevance of our results. From a practical standpoint, normalized angular defects are advocated as an estimator for the Gauss curvature in a significant number of papers—see, e.g., (Calladine, 1986; Meyer et al., 2002; Cskny and Wallace, 2000; Dyn et al., 2001). We show that the statements made in these papers are erroneous in general, although they may be true pointwise for very specific meshes. A direct consequence is that normalized angular defects should be used to estimate the Gauss curvature for these cases only where the geometry of the meshes processed is precisely controlled.

Finally, it should be emphasized that along the derivation of these results, we prove several approximation lemmas for curves and surfaces. These results may find applications in surface meshing, surface subdivision, feature extraction,

1.5. Paper overview

The paper is organized as follows. Section 2 provides the notations used throughout the paper. In Section 3 we present approximation results for the curvature of plane curves. These results are used in Section 4 to derive a formula on Euclidean triangles providing a piecewise linear approximation of a smooth surface. Using restricted hypothesis on the geometry of these triangles, we show in Section 5 that the angular defect does not provide, in general, an estimate for k_G . In Section 6, the hypothesis of Section 5 are alleviated and a general result about the accuracy of the angular defect is proved. Illustrations of the main theorems are provided in Section 7.

2. Notations

Consider a point p of a smooth surface together with n Euclidean triangles $\{p_i p p_{i+1}\}_{i=1,\dots,n}$ —with $p_{n+1} = p_1$ —forming a piecewise linear approximation of S around p . The following notations are used throughout the paper—see Fig. 3:

Normal sections; Π_i, φ_i . Consider the plane Π_i containing the normal \mathbf{n} , p and p_i . We assume Π_i is defined by its angle φ_i with respect to some coordinate system in the tangent plane—for example, the one associated with the principal directions.

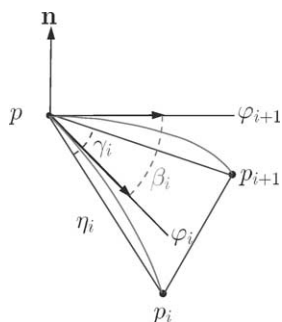


Fig. 3. Notations.

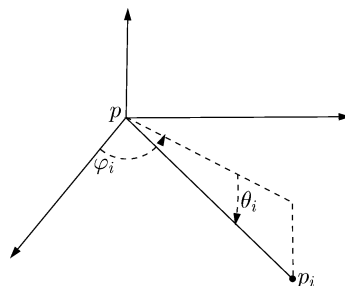


Fig. 4. p_i in spherical coordinates.

Distance to one-ring neighbor; η_i . The Euclidean distance from p to its i th neighbor p_i is denoted η_i .
Angle between normal sections; β_i . The angle between two consecutive normal sections Π_i and Π_{i+1} is denoted β_i , that is $\beta_i = \varphi_{i+1} - \varphi_i$. Put differently, β_i measures, in the tangent plane, the angle between the tangents to the plane curves $S \cap \Pi_i$ and $S \cap \Pi_{i+1}$.
Polyhedral angle; γ_i . Consider the Euclidean triangle $pp_i p_{i+1}$. The angle at p , i.e., $\angle p_i p p_{i+1}$ is denoted γ_i . (Notice that the angle γ_i is different from the angle α_i of Proposition 1.)
Directional curvatures; λ_i . We let λ_i stand for the curvature of the plane curve $S \cap \Pi_i$. Notice that if Π_i contains a principal direction, λ_i reduces to the corresponding principal curvature k_M or k_m .

3. Plane curves

In this section, we provide an estimate for the curvature of a plane curve from the angular defect of an inscribed polygon.

3.1. A lemma on plane curves

Let C be a C^∞ smooth regular curve. Let p_0 be a point of C . It is well known that C can locally be represented by the graph $(x, f(x))$ of a smooth function f , such that $p_0 = (0, 0)$ (i.e., $f(0) = 0$), and such that the tangent to C at p_0 is aligned with the x -axis (i.e., $f'(0) = 0$). Let k be the curvature of C at the origin (i.e., $k = f''(0)$), and let $v = f'''(0)$. Near the origin we have

$$f(x) = \frac{kx^2}{2} + \frac{vx^3}{6} + o(x^3). \tag{4}$$

Let us now use polar coordinates: $x = \eta \cos \theta$ and $y = \eta \sin \theta$. In order to approximate the curvature of C at p_0 , we shall need an expression of θ as a function of η . Obtaining such an expression involves the implicit function theorem, and the reader is referred to Appendix A for the proof of the following

Lemma 1. *Let $f(x)$ be a C^∞ smooth regular function with $k = f''(0)$ and $v = f'''(0)$. For a point $p = (\eta \cos \theta, \eta \sin \theta)$ on the graph of f near the origin, one has:*

$$\theta = \frac{k\eta}{2} + \frac{v\eta^2}{6} + o(\eta^2) \quad \text{if } x \geq 0, \tag{5}$$

$$\theta = \frac{k\eta}{2} - \frac{v\eta^2}{6} + o(\eta^2) \quad \text{if } x \leq 0. \tag{6}$$

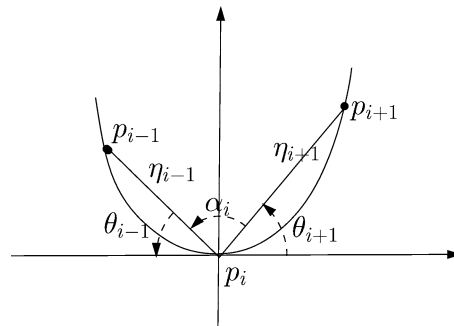


Fig. 5. Smooth curve and inscribed polygon.

3.2. Approximating the curvature of a plane curve

The previous lemma can be used to estimate the curvature of a curve from the angular defect α_i of an inscribed polygon. See Fig. 5 for the notations.

Theorem 2. Let p_{i-1} , p_i and p_{i+1} be three points as indicated on Fig. 5, with η_{i-1} (η_{i+1}) the distance from p_i to p_{i-1} (p_{i+1}). Also let $\bar{\eta}_i = (\eta_{i-1} + \eta_{i+1})/2$. The angular defect α_i at p_i and the curvature k satisfy:

- if $\eta_{i-1} = \eta_{i+1} = \eta$:

$$\frac{\pi - \alpha_i}{\eta} = k + o(\eta), \quad (7)$$

- if $\eta_{i-1} \neq \eta_{i+1}$:

$$\frac{\pi - \alpha_i}{\bar{\eta}_i} = k + o(1). \quad (8)$$

Proof. Since the proofs of the two statements are similar, we focus just on the first one.

Eqs. (5) and (6) applied to p_{i+1} and p_{i-1} yield $\theta_{i-1} + \theta_{i+1} = k\eta + o(\eta^2)$. But we also have $\theta_{i-1} + \theta_{i+1} = \pi - \alpha_i$, whence the result. \square

Interestingly, the speed of convergence is faster when the two neighbors are located at the same distance from p_i .

Remark. The previous theorem can be extended to space curves.

4. A lemma on normal sections and Euclidean triangles

This section is devoted to a general result involving Euclidean triangles and smooth surfaces. This result is the cornerstone of the next two sections.

Using the notations of Section 2, we aim at finding a dependence relationship between $\beta_i, \gamma_i, \eta_i$ and η_{i+1} . More precisely, we shall consider that the normal sections Π_i s are fixed—which determines the φ_i s, β_i s and λ_i s—and study the dependence between γ_i, η_i and η_{i+1} .

Lemma 2. *With the above notations, let $\eta = \max(\eta_i, \eta_{i+1})$. Define the following sum and product functions*

$$s(\eta_i, \eta_{i+1}) = \frac{\lambda_i^2 \eta_i^2 + \lambda_{i+1}^2 \eta_{i+1}^2}{8}, \quad p(\eta_i, \eta_{i+1}) = \frac{\lambda_i \lambda_{i+1} \eta_i \eta_{i+1}}{4}.$$

The $\beta_i, \gamma_i, \eta_i$ and η_{i+1} quantities satisfy

$$\beta_i = \gamma_i + \frac{p(\eta_i, \eta_{i+1})}{\sin \gamma_i} - s(\eta_i, \eta_{i+1}) \cot \gamma_i + o(\eta^2) \tag{9}$$

and

$$\beta_i = \gamma_i + \frac{p(\eta_i, \eta_{i+1})}{\sin \beta_i} - s(\eta_i, \eta_{i+1}) \cot \beta_i + o(\eta^2). \tag{10}$$

Proof. The proofs of the two claims following the same guideline, we just prove the second one. Assume point p is at the origin. Let us write the coordinates of p_i in spherical form with the conventions of Fig. 4—that is φ measures an angle in the tangent plane of S at p . If X^t stands for the transpose of X , the coordinates of p_i are $p_i = (\eta_i \cos \theta_i \cos \varphi_i, \eta_i \cos \theta_i \sin \varphi_i, \eta_i \sin \theta_i)^t$, and similarly for p_{i+1} .

Since $\beta_i = \varphi_{i+1} - \varphi_i$, expressing the dot product $\mathbf{pp}_i \cdot \mathbf{pp}_{i+1} = \eta_i \eta_{i+1} \cos \gamma_i$ in spherical coordinates yields

$$\cos \gamma_i = \cos \beta_i \cos \theta_i \cos \theta_{i+1} + \sin \theta_i \sin \theta_{i+1}. \tag{11}$$

Since the curve $\Pi_i \cap S$ is a plane curve, using Eq. (5) which expresses θ as a function of η , we have

$$\cos \theta_i = 1 - \frac{\lambda_i^2 \eta_i^2}{8} + o(\eta_i^2), \quad \sin \theta_i = \frac{\lambda_i \eta_i}{2} + o(\eta_i).$$

Plugging these values into Eq. (11) yields

$$\cos \gamma_i = (1 - s(\eta_i, \eta_{i+1})) \cos \beta_i + p(\eta_i, \eta_{i+1}) + o(\eta^2).$$

To turn the previous expression into a relationship between γ_i and β_i , we use the Taylor formula of order one to $f(x) = \arccos(x)$ together with $a = \cos \beta_i$ and $b = \cos \gamma_i$:

$$\gamma_i = \beta_i + \frac{-1}{\sin \beta_i} (-s(\eta_i, \eta_{i+1}) \cos \beta_i + p(\eta_i, \eta_{i+1}) + o(\eta^2)) + o(\eta^2).$$

Re-arranging the terms completes the proof. \square

5. Surfaces and regular polygons

5.1. Main result and implications

Using the lemma proved in the previous section, we are now ready to analyze the angular defect for regular meshes. We shall need the following definitions.

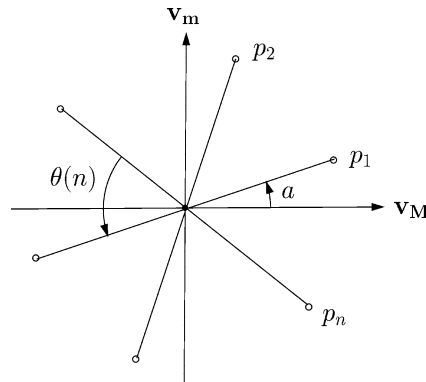


Fig. 6. Regular triangulation around p : tangent plane seen from above.

Definition 1. Let p be a point of a smooth surface S and let p_i , $i = 1, \dots, n$ be its one ring neighbors. Point p is called a *regular vertex* if (i) the p_i s lie in normal sections two consecutive of which form an angle of $\theta(n) = 2\pi/n$, (ii) the η_i s all take the same value η .

Definition 2. Consider the directions of maximum and minimum curvatures of S at p . Assume these directions are associated two vectors \mathbf{v}_M and \mathbf{v}_m such that $\mathbf{v}_M \wedge \mathbf{v}_m = \mathbf{n}$ —with \mathbf{n} be the normal of S at p . The offset angle a is defined as the angle in $[0, 2\pi[$ between the vectors \mathbf{v}_M and $\mathbf{p}\pi(\mathbf{p}_1)$ with $\pi(\mathbf{p}_1)$ the projection of p_1 in the tangent plane.

Let us now get back to the notations of Section 2 at a regular vertex. Angle a is the angle from \mathbf{v}_M to the normal section of the first normal section. For a regular vertex, the β_i s are constant and equal to $\theta(n)$, so that $\varphi_i = a + (i - 1)\theta(n)$. Under these hypothesis, we provide a closed form expression for the angular defect. The reader is referred to Appendix B for the proof of the following theorem.

Theorem 3. Consider a regular vertex of valence n . The following holds:

(1) There exists two functions $A(a, n)$ and $B(a, n)$ such that

$$2\pi - \sum_{i=1}^n \gamma_i = [A(a, n)k_G + B(a, n)(k_M^2 + k_m^2)]\eta^2 + o(\eta^2). \quad (12)$$

(2) The only value of n such that the functions $A(a, n)$ and $B(a, n)$ depend upon a is $n = 4$, and then

$$2\pi - \sum_{i=1}^n \gamma_i = [(1 - 2\cos^2 a \sin^2 a)k_G + \cos^2 a \sin^2 a(k_M^2 + k_m^2)]\eta^2 + o(\eta^2). \quad (13)$$

(3) If $n \neq 4$:

$$2\pi - \sum_{i=1}^n \gamma_i = \frac{n}{16 \sin 2\pi/n} \left[\left(2 - \cos \frac{4\pi}{n} - \cos \frac{2\pi}{n} \right) k_G + \left(1 + \frac{1}{2} \cos \frac{4\pi}{n} - \frac{3}{2} \cos \frac{2\pi}{n} \right) (k_M^2 + k_m^2) \right] \eta^2 + o(\eta^2). \quad (14)$$

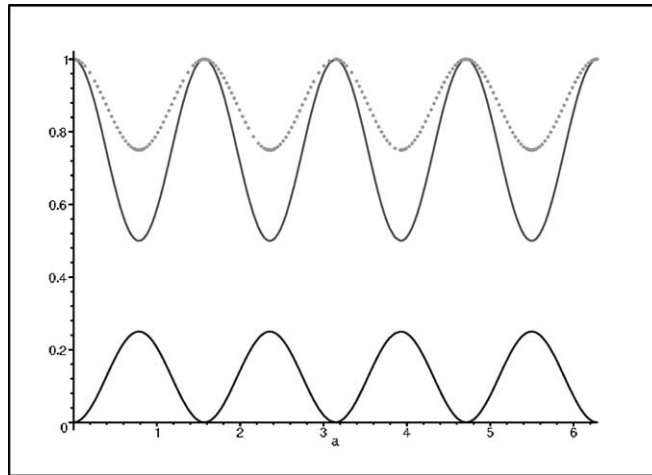


Fig. 7. The coefficients $A(a, 4)$, $B(a, 4)$ and $A(a, 4) + B(a, 4)$ —respectively (solid curve, top), (solid curve, bottom), (dotted curve).

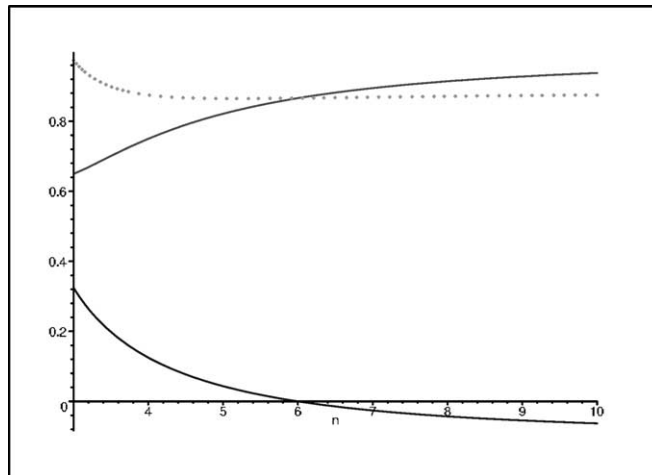


Fig. 8. The coefficients $A(a, n)$, $B(a, n)$ and $A(a, n) + B(a, n)$ —respectively (solid curve, top), (solid curve, bottom), (dotted curve).

In particular, the only value of n such that $B(a, n) = 0$ is $n = 6$, and then $A(a, 6) = \sqrt{3}/2$, that is

$$2\pi - \sum_i \gamma_i = \frac{\sqrt{3}}{2} k_G \eta^2 + o(\eta^2). \tag{15}$$

The graphs of the functions $A(a, 4)$ and $B(a, 4)$, as well as $A(a, n)$ and $B(a, n)$ for $n \neq 4$ are presented on Figs. 7 and 8. For the angular defect to provide an estimate for k_G , a sufficient condition is to have a regular triangulation of valence $n = 4$ with the one-ring neighbors are aligned with the principal directions. Another sufficient condition is to have a regular valence six triangulation. Therefore, the angular defect is expected to provide good results for triangulations where valence six vertices are

prominent. Example such triangulations are those generated by subdivision processes. Apart from the two favorable configurations just mentioned, several other configurations are of course possible. From a practical standpoint, these results show that normalized angular defects should be used to estimate the Gauss curvature for these cases only where the geometry of the meshes processed is precisely controlled.

The *valence six almost everywhere* observation is also related to the following question. In Section 1.2 we recalled the Gauss–Bonnet theorem for a polyhedra P and a compact orientable surface S . Assume P and S are homeomorphic. An interesting issue is the global convergence of the sum of the angular defects over P when P is refined so as to converge to S . The fact that valence six vertices are expected almost everywhere is certainly related to the answer. Fully resolving this issue is a geometric measure theory related question.

At last, the previous theorem fully explains the observation made in (Meek and Walton, 2000), based on a counter-example, that the angular defect does not estimate the Gauss curvature.

5.2. Corollaries

Interestingly, although the Gauss curvature is not estimated by the angular defect, the principal curvatures can be recovered from two different meshes:

Corollary 1. *The principal curvatures of a smooth surface can be computed from the angular defects of any two meshes of valences n_1 and n_2 such that $n_1 \neq 4$, $n_2 \neq 4$, $n_1 \neq n_2$.*

In particular, consider a sequence T_{2p} of triangulations of valence $2p$ with $p \geq 3$ and $p \neq 4$. Let T_p be any regular sequence of sub-triangulations of T_{2p} . (That is any triangulation in T_p is regular in the usual sense.) The principal curvatures can be computed from the angular defects of T_{2p} and T_p .

Proof. Assume we are given two meshes with valences n_1 and n_2 different from four. Let $E(n_i)$ be the limit value of $(2\pi - \sum_i \gamma_i)/\eta^2$, and $A(n_i)$, $B(n_i)$ be the coefficients of k_G and $k_m^2 + k_M^2$ in Eq. (12) have:

$$\begin{cases} E(n_1) = A(n_1)k_G + (k_m^2 + k_M^2)B(n_1), \\ E(n_2) = A(n_2)k_G + (k_m^2 + k_M^2)B(n_2). \end{cases}$$

Since $n_1 \neq n_2 \Rightarrow A(n_1)B(n_2) - A(n_2)B(n_1) \neq 0$, we have

$$k_G = \frac{E(n_1)B(n_2) - E(n_2)B(n_1)}{A(n_1)B(n_2) - A(n_2)B(n_1)}. \quad (16)$$

If E refers to one of the $E(n_i)$ and similarly for A and B , once the Gauss curvature is known, we are left with the system

$$\begin{cases} k_m k_M = k_G, \\ (k_m^2 + k_M^2)B = E - Ak_G. \end{cases}$$

Letting $D = E - Ak_G$ and observing that $B \neq 0$ since $n \neq 4$ yields

$$Bk_m^4 - Dk_m^2 + Bk_G^2 = 0, \quad (17)$$

which solves to

$$k_m^2 = \frac{E - Ak_G - \sqrt{(E - Ak_G)^2 - 4B^2k_G^2}}{2B}. \quad (18)$$

Notice that the sign of the square root chosen in the previous expression does not matter since the two solutions corresponding to $\pm\sqrt{}$ are actually conjugated with respect to $k_m k_M = k_G$, that is

$$k_M^2 = \frac{k_G^2}{k_m^2} = \frac{E - Ak_G + \sqrt{(E - Ak_G)^2 - 4B^2k_G^2}}{2B}. \tag{19}$$

Once k_m^2 and k_M^2 have been computed, k_m and k_M are determined observing that the product of their signs is the sign of k_G , and that $k_m \leq k_M$. Once k_m and k_M are known, the mean curvature k_H is $k_H = (k_m + k_M)/2$.

For the second part, just apply the first part to the two regular sequences of triangulations T_{2p} and T_p . \square

In the same spirit, we also have:

Corollary 2. *Umbilics can be detected from the two angular defects without computing the principal curvatures.*

Proof. At an umbilic point, we have $k_m = k_M$. Using the notations of the previous proof, it is easily checked that $(E - Ak_G)^2 - 4B^2k_G^2 = 0$ and $\text{sign}(k_G) \geq 0$. \square

Since two meshes are enough to infer the principal curvatures, it is tempting to infer the position of the principal directions using the valence four mesh and Eq. (13). This equation yields the value of $\cos^2 a \sin^2 a$, from which one is unable to distinguish between a and $2\pi - a$.

Remark. It is important to notice that Corollary 1 compares the Gauss curvature and the squares of the principal curvatures of S against the angular defect normalized by η^2 —see Section 1.2 for a discussion of the dimensionality issues.

6. Surfaces: the general case

This section generalizes the analysis carried out in the previous section. We relax the hypothesis on the edges' lengths η_i s as well as on the angles φ_i s, and provide an expression of the angular defect as a Taylor expansion in the edges' lengths.

6.1. Angular defect and k_G

We shall need the following definition:

Definition 3. Consider the one-ring neighbors of p . For the sake of conciseness, let $c_i = \cos \varphi_i$, $s_i = \sin \varphi_i$, and define the following quantities:

$$A_i = \frac{1}{4 \sin \gamma_i} \left[\eta_i \eta_{i+1} (c_i^2 s_{i+1}^2 + s_i^2 c_{i+1}^2) - \frac{\cos \gamma_i}{2} (\eta_i^2 (2c_i^2 s_i^2) + \eta_{i+1}^2 (2c_{i+1}^2 s_{i+1}^2)) \right], \tag{20}$$

$$B_i = \frac{1}{4 \sin \gamma_i} \left[\eta_i \eta_{i+1} (c_i^2 c_{i+1}^2) - \frac{\cos \gamma_i}{2} (\eta_i^2 c_i^4 + \eta_{i+1}^2 c_{i+1}^4) \right], \quad (21)$$

$$C_i = \frac{1}{4 \sin \gamma_i} \left[\eta_i \eta_{i+1} (s_i^2 s_{i+1}^2) - \frac{\cos \gamma_i}{2} (\eta_i^2 s_i^4 + \eta_{i+1}^2 s_{i+1}^4) \right], \quad (22)$$

$$S_p = A + B + C \quad \text{with } A = \sum_i A_i, \quad B = \sum_i B_i, \quad C = \sum_i C_i. \quad (23)$$

The quantity S_p is called the *module* of the mesh at p .

The first lemma we shall need is about the independence of the module with respect to the positions of the normal sections:

Lemma 3. *The module of the mesh at p is independent from the angles $\varphi_1, \dots, \varphi_n$.*

Proof. Simply observe that

$$A_i + B_i + C_i = \frac{1}{4 \sin \gamma_i} \left[\eta_i \eta_{i+1} - \frac{\cos \gamma_i}{2} (\eta_i^2 + \eta_{i+1}^2) \right]. \quad \square$$

The second lemma states, as in the regular case, that the angular defect is a homogeneous polynomial of degree two in the principal curvatures:

Lemma 4. *Let $\eta = \sup_i \eta_i$. The angular defect and the principal curvatures satisfy*

$$2\pi - \sum_{i=1}^n \gamma_i = (Ak_G + Bk_M^2 + Ck_m^2) + o(\eta^2). \quad (24)$$

Proof. We express the directional curvature λ_i using Euler's relation. Plugging the values of λ_i and λ_{i+1} into Eq. (9), summing over the n one-ring neighbors and grouping terms in k_G , k_M^2 and k_m^2 yields Eq. (24). \square

The main result, at last, provides an upper bound for the discrepancy between the normalized angular defect and the Gauss curvature:

Theorem 4. *Let T_m be a sequence of meshes on a surface having p as a common vertex. Consider the one-ring around p . Let $\bar{\eta}_m = \sup_i \eta_{m_i}$, $\underline{\eta}_m = \inf_i \eta_{m_i}$. Suppose that*

- (1) *there exist two positive constants $\gamma_{\min}, \gamma_{\max}$ such that $\forall i, \forall m, 0 < \gamma_{\min} \leq \gamma_{m_i} \leq \gamma_{\max}$.*
- (2) *there exist two positive constants η_1, η_2 such that $\forall m, \eta_1 \leq \bar{\eta}_m / \underline{\eta}_m \leq \eta_2$.*

Then, there exists a positive constant C such that

$$\limsup_m \left| \frac{2\pi - \sum_i \gamma_{i_m}}{S_{p_m}} - k_G \right| \leq \frac{nC}{2 \sin \gamma_{\min}} [(k_M - k_m)^2 + |k_M^2 - k_m^2|]. \quad (25)$$

Proof. Let us consider a particular mesh in the sequence, and for the sake of clarity, let us omit its index m . We have $B_i \leq \eta^2/(2 \sin \gamma_i)$ whence $B \leq n\eta^2/(2 \sin \gamma_i)$. The same inequalities hold for C_i and C . From Eq. (24), we get

$$\begin{aligned} \left| 2\pi - \sum_i \gamma_i - (A + B + C)k_G \right| &= \left| B(k_M^2 - k_G) + C(k_m^2 - k_G) \right| + o(\eta^2) \\ &= \left| \frac{B + C}{2}(k_M - k_m)^2 + \frac{B - C}{2}(k_M^2 - k_m^2) \right| + o(\eta^2) \\ &\leq \frac{B + C}{2}(k_M - k_m)^2 + \left| \frac{B - C}{2} \right| |k_M^2 - k_m^2| + o(\eta^2). \end{aligned} \tag{26}$$

Using the upper bounds on B and C and since S_p does not depend on the angles $\varphi_1, \dots, \varphi_n$, we get:

$$\left| \frac{2\pi - \sum_i \gamma_i}{S_p} - k_G \right| \leq \frac{\eta^2}{|S_p|} \frac{n}{2 \sin \gamma_{\min}} ((k_M - k_m)^2 + |k_M^2 - k_m^2|) + o(1). \tag{27}$$

Let us now get back to the sequence of meshes, i.e., consider that the previous equation is indexed by m —that is $\eta = \bar{\eta}_m$, $\gamma_i = \gamma_{m_i}$, $S_p = S_{p,m}$. The assumptions on the γ_{m_i} angles and those on $\bar{\eta}_m/\underline{\eta}_m$ imply that there exists a constant \mathcal{C} such that $\eta^2/|S_p| \leq \mathcal{C}$, whence the result. \square

The previous theorem deserves several comments:

- The lim sup accounts for the fact that the limit of the discrepancy between the normalized angular defect and k_G may not exist. The hypothesis used make it bounded, but one may have a sequence of alternating triangulations (e.g., indexed by odd and even integers) with different properties.
- Theorem 4 shows that the error uncured when approximating the Gauss curvature by $(2\pi - \sum_i \gamma_i)/S_p$ depends upon k_M and k_m . In particular, this error is minimum if $k_M = k_m$ if $k_G > 0$ —or $k_M = -k_m$ if $k_G < 0$. Although the Gauss curvature is intrinsic, i.e., invariant upon isometric transformations of the surface, the accuracy of the estimate depends upon the particular embedding considered.
- In using geodesic triangulations to estimate k_G , the natural quantity to divide the angular defect by is the area of the triangles surrounding p . As the previous analysis shows, using Euclidean triangles induces the module of the mesh rather than its area. (Notice however that in both cases, the denominator is homogeneous to a surface area.)
- It should be observed that the error term may vanish under very special circumstances. We have encountered two of them in Section 5, namely for a valence six triangulation, or a valence four triangulation with $a = 0 \pmod{\pi/2}$. Other cancellations can certainly be obtained exploiting the independence of the η_i s and the φ_i s.

6.2. Angular defect and the second fundamental form

We proceed with a couple of examples illustrating the relationship between the angular defect, the Gauss curvature and the second fundamental form.

Example 1. Consider the monkey saddle of Fig. 9, point p being at the origin. Using a triangulation whose one-ring neighbors are located above or below the $z = 0$ plane results in a positive angular defect—as if we were processing an elliptic vertex. Using a triangulation whose points are distributed on the two

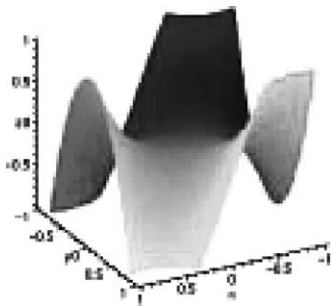


Fig. 9. Monkey saddle.

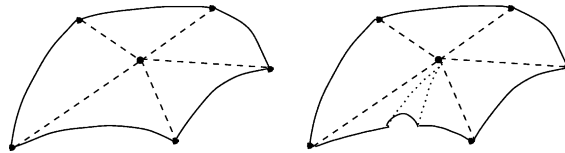


Fig. 10. Local fold.

sides of the tangent plane results in a negative angular defect—as if an hyperbolic vertex was processed. Does this mean that two different triangulations may yield Gauss curvatures with opposite signs?

Fortunately not! For a surface such as the Monkey saddle, the second fundamental form II_p is null so that the point is a planar point and any directional curvature around p is also null. No matter what triangulation is used, the angular defect will converge to zero which corresponds to a null Gauss curvature.

Example 2. Consider now the two surfaces of Fig. 10 and assume they differ by a small “fold” located in-between two consecutive one-ring neighbors of the mesh. If II_p does not change—the fold affects third or higher order terms of the Monge form of S at p , neither the directional curvatures nor the angular defect are affected.

7. Illustrations

7.1. Experimental setup

This section discusses two examples illustrating the theoretical results of Sections 5 and 6. Since all the properties we care about are second order differential properties, we focus on degree two surfaces near a given point—taken to be the origin without loss of generality. We assume the surfaces are given as height functions in the coordinate system associated with the principal directions and the normal, and we study experimentally the normalized angular defect for a sequence of triangulations converging to the origin.

With the usual notations, the surface is locally the graph of the bivariate function

$$z = \frac{1}{2}(k_M x^2 + k_m y^2). \tag{28}$$

Let p be a point on the surface and denote (x, y, z) its coordinates. Using polar coordinates in the tangent plane, that is $(x, y, z) = (r \cos \theta, r \sin \theta, z(x, y))$, and using Euler’s relation, Eq. (28) also reads as

$$z = \frac{1}{2}k_v r^2,$$

with k_v the directional curvature in the normal section at angle θ . The square distance η^2 between the origin and the point $p(x, y, z)$ satisfies

$$\eta^2 = r^2 + \left(\frac{1}{2}k_v r^2\right)^2,$$

or equivalently,

$$r^2 = \frac{2(-1 + \sqrt{1 + \eta^2 k_v^2})}{k_v^2}. \tag{29}$$

From the previous equation and once θ has been set, one easily computes the coordinates of the point p lying in the normal section at angle θ and at distance η from the origin. Repeating this operation for n pairs $(\theta_i, \eta_i)_{i=1, \dots, n}$ defines the triangulation we are interested in. We shall consider three different sequences of triangulations:

Scenario #1: the regular case The angles and the edges' lengths are chosen as in Section 5. The sequence of triangulations is parameterized by η , the common edge length.

Scenario #2 The angles are chosen as is the regular case, but the edges' lengths are chosen uniformly at random in the range $[0, \eta]$. More precisely and in order to be able to study the convergence over the sequence, we assume that for each one-ring neighbor and whatever the value of η , we have $\eta_i = r d_i \eta$ with $r d_i$ a random number in $[0, 1]$.

Scenario #3 The angles are chosen at random but the edges' lengths are all equal to η . As in the previous case and in order to be able to study the convergence over the sequence, the angles φ_i are chosen once for all for the n one-ring neighbors.

The statistics considered over a sequence of triangulations are the following ones:

- the angular defect $\delta = 2\pi - \sum_{i=1}^n \gamma_i$,
- the normalized angular defect δ/η^2 ,
- the expected limit L of the normalized angular defect as stated in Theorem 3 for the regular case and in Lemma 4 for the general case.

7.2. Experimental results

As a first example, we present convergence results of regular triangulations for the elliptic paraboloid $z = (2x^2 + y^2)/2$. Tables 1 and 2 present the results for a sequence of uniform valence six and eight triangulations. For the valence eight triangulations, three such triangulations with decreasing edges' lengths are displayed on Fig. 11.

In both cases and when the edges' lengths tend to zero, the triangles get flatter and the angular defect converges to zero. The convergence rate is captured upon re-normalization by η^2 , and one indeed observes

Table 1
Convergence of the angular defect. Surface:
 $z = (2x^2 + y^2)/2$; Scenario #1, $n = 6$

η	δ	δ/η^2	L
1.000	0.97151	0.97151	1.73205
0.500	0.35429	1.41716	1.73205
0.100	0.01716	1.71563	1.73205
0.010	0.00017	1.73188	1.73205
0.001	0.00000	1.73205	1.73205

Table 2
Convergence of the angular defect. Surface:
 $z = (2x^2 + y^2)/2$; Scenario #1, $n = 8$

η	δ	δ/η^2	L
1.000	0.91462	0.91462	1.61396
0.500	0.33104	1.32416	1.61396
0.100	0.01599	1.59887	1.61396
0.010	0.00016	1.61381	1.61396
0.001	0.00000	1.61396	1.61396

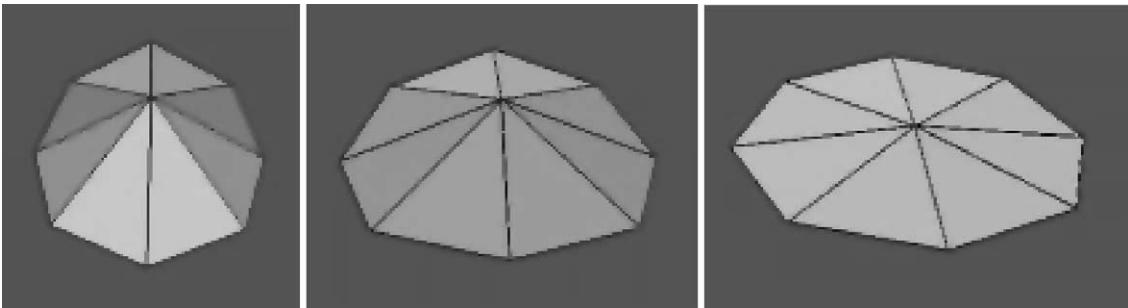


Fig. 11. A sequence of valence $n = 8$ regular triangulations for the elliptic paraboloid $z = (2x^2 + y^2)/2$. The normalized angular defect does not converge to the Gauss curvature— $k_G = 2$ for this example.

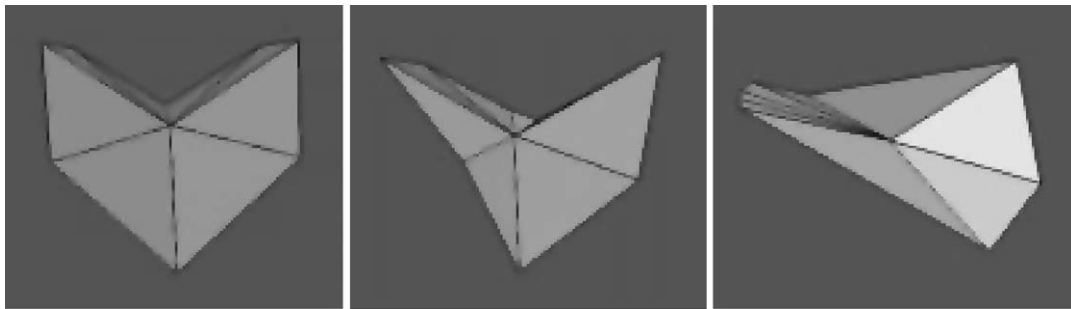


Fig. 12. Triangulations of the hyperbolic paraboloid $z = (2x^2 - y^2)/2$: (a) Regular triangulation; (b) Uniform angles but random edges' lengths; (c) Random angles and uniform edges' lengths. The normalized angular defects computed over such sequences converge to different limits depending upon k_G but also k_m^2 and k_M^2 .

Table 3
Convergence of the angular defect. Surface: $z = (2x^2 - y^2)/2$; Scenario #2, $n = 8$

η	δ	δ/η^2	L
1.000	-0.77612	-0.77612	-0.83335
0.500	-0.26690	-1.06758	-1.06824
0.100	-0.01247	-1.24723	-1.24629
0.010	-0.00013	-1.25667	-1.25666
0.001	-0.00000	-1.25677	-1.25677

Table 4
Convergence of the angular defect. Surface: $z = (2x^2 - y^2)/2$; Scenario #3, $n = 8$

η	δ	δ/η^2	L
1.000	-0.69576	-0.69576	-1.09207
0.500	-0.26373	-1.05492	-1.24080
0.100	-0.01346	-1.34561	-1.35641
0.010	-0.00014	-1.36311	-1.36322
0.001	-0.00000	-1.36329	-1.36329

that δ/η^2 converges to the expected limit. The sequence of valence six triangulations provides, up to a $\sqrt{3}/2$ factor, the exact value for k_G . The valence eight triangulations does not since the limit value involves the squares of the principal curvatures.

A second example is provided by the two sequences of triangulations of the hyperbolic paraboloid $z = (2x^2 - y^2)/2$ —see Fig. 12 (b), (c). These triangulations correspond to scenarios #2 and #3 of the previous section. For scenario #2 and since we assume the ratio of any pair of edges lengths η_i/η_j is fixed over the sequence when η decreases, it still makes sense to consider the normalized angular defect, whose limit value is given by Lemma 4. For scenario #3, the normalized angular defect also makes sense

since $\eta_i = \eta$ for all one-ring neighbors. The results are displayed on Tables 3 and 4. The concordance between the computed value and the theoretical one is that expected. The limits associated with the two triangulations are different and involve the squares of the principal curvatures.

8. Conclusion

Let S be a smooth surface, p a point of S , and consider a mesh providing a piecewise linear approximation of S around p . This paper establishes, asymptotically, several approximation results relating the curvatures of S at p and normalized angular defects of meshes at p . In particular, we show that the angular defect does not provide in general, an accurate point-wise estimate of the Gauss curvature.

From a practical standpoint, these results show that normalized angular defects should be used to estimate the Gauss curvature for these cases only where the geometry of the meshes processed is precisely controlled. From a theoretical perspective, we believe these contributions might find applications for the many operations involving differential operators on meshes, that is fairing, smoothing, as well as subdivision. A clear understanding of the geometry of meshes in certainly one step forward more robust algorithms.

On a broader perspective, these contributions illustrate the difficulties one has to face in order to perform *differential geometry* on non smooth objects. It would therefore be very interesting to generalize the analysis presented in this paper to all the methods—least-square quadrics, gradient-based operators, etc.—which are used to estimate the normal, mean curvature, principal directions, ridges, etc of triangulated surfaces.

Acknowledgements

The authors wish to thank Sylvain Petitjean for rereading this paper.

Appendix A. Proof of Lemma 1

Using spherical coordinates ($x = \eta \cos \theta$, $y = \eta \sin \theta$) to express the position of a point $p \in C$, we get that C is implicitly represented by $F(\eta, \theta) = 0$ with

$$F(\eta, \theta) = y - f(x) = \eta \sin \theta - f(\eta \cos \theta). \quad (\text{A.1})$$

Obtaining an expression of θ as a function of η involves the implicit function theorem applied to F at $(\eta = 0, \theta = 0)$. Unfortunately, $\partial F / \partial \theta(0, 0) = 0$. We get around the difficulty using an auxiliary function Φ defined as follows:

Lemma 5. Let $\Phi(\eta, \theta)$ be defined by

$$\eta \neq 0: \quad \Phi(\eta, \theta) = \frac{F(\eta, \theta)}{\eta} = \sin \theta - \frac{f(\eta \cos \theta)}{\eta}, \quad (\text{A.2})$$

$$\eta = 0: \quad \Phi(0, \theta) = \sin \theta. \quad (\text{A.3})$$

The function Φ is C^2 , and the point $(\eta = 0, \theta = 0)$ is a regular point of Φ . Moreover, near the origin

$$\theta = A\eta + B\eta^2 + o(\eta^2).$$

Proof. The proof consists of three parts.

Part I. $\Phi(\eta, \theta)$ versus $F(\eta, \theta)$. We first observe that working with $F(\eta, \theta)$ or $\Phi(\eta, \theta)$ is equivalent. When $\eta \neq 0$, the solutions of $F = 0$ and $\Phi = 0$ are the same. If $\eta = 0$, the only solution of $\Phi = 0$ is $(0, \theta = 0)$ which is also a solution of $F = 0$. To be more precise, any pair $(0, \theta)$ is a solution of $F = 0$, and working with Φ instead of F retains only one of these solutions, namely $(0, 0)$.

Part II. $\Phi(\eta, \theta)$ is C^2 . To begin with, observe that

$$f(x) = kx^2/2 + vx^3/6 + o(x^3) \quad \text{and} \quad f'(x) = kx + vx^2/2 + o(x^2).$$

Using these two expressions in the following calculations are straightforward.

Φ is C^0 .

$$\lim_{\eta \rightarrow 0} \frac{F(\eta, \theta)}{\eta} = \lim_{\eta \rightarrow 0} \sin \theta - f(\eta \cos \theta) = \sin \theta.$$

Φ is C^1 . We consider $\partial\Phi/\partial\eta(0, \theta)$ and $\partial\Phi/\partial\theta(0, \theta)$ in the two settings— $\eta \neq 0$ and $\eta = 0$.

- $\eta \neq 0, \partial\Phi/\partial\eta(0, \theta)$

$$\frac{\partial\Phi}{\partial\eta}(0, \theta) = \lim_{\eta \rightarrow 0} \frac{\partial\Phi}{\partial\eta}(\eta, \theta) = -\frac{k \cos^2 \theta}{2}.$$

- $\eta = 0, \partial\Phi/\partial\eta(0, \theta)$

$$\frac{\partial\Phi}{\partial\eta}(0, \theta) = \lim_{\eta \rightarrow 0} \frac{\Phi(\eta, \theta) - \Phi(0, \theta)}{\eta} = \lim_{\eta \rightarrow 0} \left(\sin \theta - \frac{f(\eta \cos \theta)}{\eta} - \sin \theta \right) = -\frac{k \cos^2 \theta}{2}.$$

- $\eta \neq 0, \partial\Phi/\partial\theta(0, \theta)$

$$\frac{\partial\Phi}{\partial\theta}(0, \theta) = \lim_{\eta \rightarrow 0} \frac{\partial\Phi}{\partial\theta}(\eta, \theta) = \cos \theta.$$

- $\eta = 0, \partial\Phi/\partial\theta(0, \theta)$

$$\frac{\partial\Phi}{\partial\theta}(0, \theta) = \frac{\partial \sin \theta}{\partial \theta}(0, \theta) = \cos \theta.$$

Φ is C^2 . The equality of the four second order derivatives $\partial^2\Phi/(\partial u^1 \partial u^2)$ with $u^1 = \{\eta, \theta\}$ and $u^2 = \{\eta, \theta\}$ in the two settings are checked similarly.

Part III. Expression of θ as a function of (η) . To see that $(0, 0)$ is a regular point, observe that $\partial\Phi/\partial\theta(0, 0) = \cos 0 = 1$. Since Φ is C^2 , applying the implicit function theorem yields

$$\theta = A\eta + B\eta^2 + o(\eta^2). \quad \square$$

The proof of lemma is now straightforward:

Proof. From Eq. (9), one easily derives the equivalents of $\cos \theta$ and $\sin \theta$ as a function of η . Plugging them into Eq. (4) yields Eq. (5). Eq. (6) is proved in the same way observing that $p_{i-1} = (-\eta_{i-1} \cos \theta_{i-1}, \eta_{i-1} \sin \theta_{i-1})$. \square

Appendix B. Proof of Theorem 3

The proof of Theorem 3 consists of working out the expressions of $A(a, n)$, $B(a, n)$ and $C(a, n)$ from Eq. (10). We begin with a lemma about trigonometric sums.

Lemma 6. Define the three trigonometric sums

$$\begin{aligned}
 t_1(a, n) &= \sum_{i=1}^n \cos(2\varphi_i), \\
 t_2(a, n) &= \frac{1}{2} \sum_{i=1}^n \cos(2\varphi_i + 2\varphi_{i-1}), \\
 t_3(a, n) &= \sum_{i=1}^n \cos(4\varphi_i).
 \end{aligned}
 \tag{B.1}$$

For a regular uniform mesh of valence n , we have

$$2\pi - \sum_{i=1}^n \gamma_i = [A(a, n)k_G + B(a, n)k_M^2 + C(a, n)k_m^2]\eta^2 + o(\eta^2)
 \tag{B.2}$$

with

$$A(a, n) = \frac{1}{16 \sin \theta(n)} (2n - n \cos 2\theta(n) - n \cos \theta(n) - t_2(a, n) + t_3(a, n) \cos \theta(n)),
 \tag{B.3}$$

$$\begin{aligned}
 B(a, n) &= \frac{1}{16 \sin \theta(n)} \left(n + \frac{n}{2} \cos 2\theta(n) - \frac{3n}{2} \cos \theta(n) + 2(1 - \cos \theta(n))t_1(a, n) \right. \\
 &\quad \left. + t_2(a, n) - \frac{\cos \theta(n)}{2} t_3(a, n) \right),
 \end{aligned}
 \tag{B.4}$$

$$\begin{aligned}
 C(a, n) &= \frac{1}{16 \sin \theta(n)} \left(n + \frac{n}{2} \cos 2\theta(n) - \frac{3n}{2} \cos \theta(n) - 2(1 - \cos \theta(n))t_1(a, n) \right. \\
 &\quad \left. + t_2(a, n) - \frac{\cos \theta(n)}{2} t_3(a, n) \right).
 \end{aligned}
 \tag{B.5}$$

Proof. Since the angles in the tangent plane are known, we work out the angular defect using Eq. (10) rather than Eq. (9). Assuming that $\eta_i = \eta$ and $\beta_i = \theta(n)$, we rewrite Eq. (10) as follows:

$$\frac{4 \sin \theta(n)}{\eta^2} (\beta_i - \gamma_i) = \mu_i + o(1)
 \tag{B.6}$$

with

$$\mu_i = \lambda_i \lambda_{i+1} - \frac{1}{2} (\lambda_i^2 + \lambda_{i+1}^2) \cos \theta(n).
 \tag{B.7}$$

Expressing the directional curvatures λ_i with Euler’s relation, that is

$$\lambda_i = \cos^2 \varphi_i k_M + \sin^2 \varphi_i k_m,
 \tag{B.8}$$

and substituting into $\sum_{i=1}^n \mu_i$ yields a homogeneous polynomial of degree four in sines and cosines. We linearize this polynomial using the standard formulae $\cos^2 a = (1 + \cos 2a)/2$, $\sin^2 a = (1 - \cos 2a)/2$, $\cos a \cos b = (\cos(a+b)/2 + \cos(a-b))/2$, as well as $\cos^2 a \sin^2 a = (1 - \cos 4a)/8$, $\cos^4 a = (\cos 4a + 4 \cos 2a + 3)/8$, $\sin^4 a = (\cos 4a - 4 \cos 2a + 3)/8$. These calculations simplify to Eqs. (B.3), (B.4) and (B.5).

Notice that the expressions of $B(a, n)$ and $C(a, n)$ just differ by the sign of the coefficient of $t_1(a, n)$. \square

Lemma 7. Let α and β be positive integers, and consider the sum

$$S(\alpha, \beta, n) = \sum_{k=1}^n \cos\left(\alpha + k \frac{\beta\pi}{n}\right). \quad (\text{B.9})$$

If $\beta\pi/n = 0 \pmod{2\pi}$, then $S(\alpha, \beta, n) = n \cos \alpha$. If $\beta\pi/n \neq 0 \pmod{2\pi}$ and $\beta\pi = 0 \pmod{2\pi}$, then $S(\alpha, \beta, n) = 0$.

Proof. If $\beta\pi/n = 0 \pmod{2\pi}$, the result is trivial. Otherwise, consider the two terms:

$$S(\alpha, \beta, n) = \sum_{k=1}^n \cos\left(\alpha + k \frac{\beta\pi}{n}\right), \quad T(\alpha, \beta, n) = \sum_{k=1}^n \sin\left(\alpha + k \frac{\beta\pi}{n}\right). \quad (\text{B.10})$$

Let $\beta(n) = \beta\pi/n$. Using complex numbers we have the geometric sum

$$S(\alpha, \beta, n) + iT(\alpha, \beta, n) = \sum_{k=1}^n e^{i\alpha} (e^{i\beta(n)})^k = e^{i(\alpha+\beta(n))} \frac{1 - e^{in\beta(n)}}{1 - e^{i\beta(n)}} \quad (\text{B.11})$$

whose numerator is null if $n\beta(n) = \beta\pi = 0 \pmod{2\pi}$. \square

We are now ready to prove Theorem 3:

Proof. To prove (1), we need to show that $B(a, n) = C(a, n)$ in Lemma 6. Using the trigonometric sum of Lemma 7, we have $t_1(a, n) = S(2a, 4, n)$, $t_2(a, n) = S(4a - 4\pi/n, 8, n)$, $t_3(a, n) = S(4a, 8, n)$.

But $t_1(a, n) = 0$ for all values of n since, by the same lemma, we never have $4\pi/n = 0 \pmod{2\pi}$ for $n \geq 3$. Since B and C just differ by the sign of the coefficient of t_1 , $B = C$ for all ns .

For (2), $A(a, n)$ and $B(a, n)$ depend upon a if the trigonometric sums t_2 or t_3 are non vanishing. According to the above lemma the condition is $8\pi/n = 0 \pmod{2\pi}$, which occurs for $n = 4$ only.

For (3), it is easily checked that the only value of n such that $B(a, n)$ vanishes is $n = 6$. \square

References

- Amenta, N., Bern, M., 1999. Surface reconstruction by Voronoi filtering. *Discrete Comput. Geom.* 22 (4), 481–504.
- Banchoff, T.F., 1967. Critical points and curvature for embedded polyhedra. *J. Differential Geom.* 1, 245–256.
- Calladine, C.R., 1986. Gaussian curvature and shell structures. In: Gregory, J.A. (Ed.), *The Mathematics of Surfaces*. Oxford Univ. Press.
- Cheeger, J., Müller, W., Schrader, R., 1984. On the curvature of piecewise flat spaces. *Comm. Math. Phys.* 92.
- Cskny, P., Wallace, A.M., 2000. Computation of local differential parameters on irregular meshes. In: Cipolla, R., Martin, R. (Eds.), *Mathematics of Surfaces*. Springer.

- Dyn, N., Hormann, K., Kim, S.-J., Levin, D., 2001. Optimizing 3d triangulations using discrete curvature analysis. In: Lyché, T., Shumaker, L.L. (Eds.), *Mathematical Methods for Curves and Surfaces*. Vanderbilt Univ. Press.
- Lafontaine, J., 1986. Mesures de courbures des variétés lisses et discrètes. Sem. Bourbaki 664.
- Meyer, M., Desbrun, M., Schröder, P., Barr, A.H., 2002. Discrete differential-geometry operators for triangulated 2-manifolds. In: *VisMath*.
- Morvan, J.-M., Thibert, B., 2001. Smooth surface and triangular mesh: Comparison of the area, the normals and the unfolding. In: *ACM Symposium on Solid Modeling and Applications*.
- Meek, D.S., Walton, D.J., 2000. On surface normal and Gaussian curvature approximations given data sampled from a smooth surface. *Comput. Aided Geom. Design*.
- Polthier, K., Schmies, M., 1998. Straightest geodesics on polyhedral surfaces. In: Hege, H.C., Polthier, K. (Eds.), *Mathematical Visualization*.
- Reshetnyak, Y.G., 1993. Two-dimensional manifolds of bounded curvature. In: Reshetnyak, Y.G. (Ed.), *Geometry IV*. In: *Encyclopedia of Mathematical Sciences*, Vol. 70. Springer, Berlin.
- Spivak, M., 1999. *A Comprehensive Introduction to Differential Geometry*, 3rd edn. Publish or Perish.
- Taubin, G., 1995. Estimating the tensor of curvature of a surface from a polyhedral approximation. In: *15th International Conference on Computer Vision*.
- Watanabe, K., Belyaev, A.G., 2001. Detection of salient curvature features on polygonal surfaces. In: *Eurographics*.